

# Relational Representation Distillation

Nikolaos Giakoumoglou  
Imperial College London  
London, UK, SW7 2AZ

n.giakoumoglou23@imperial.ac.uk

Tania Stathaki  
Imperial College London  
London, UK, SW7 2AZ

t.stathaki@imperial.ac.uk

## Abstract

*Knowledge distillation (KD) is an effective method for transferring knowledge from a large, well-trained teacher model to a smaller, more efficient student model. Despite its success, one of the main challenges in KD is ensuring the efficient transfer of complex knowledge while maintaining the student’s computational efficiency. Unlike previous works that applied contrastive objectives promoting explicit negative instances, we introduce Relational Representation Distillation (RRD). Our approach leverages pairwise similarities to explore and reinforce the relationships between the teacher and student models. Inspired by self-supervised learning principles, it uses a relaxed contrastive loss that focuses on similarity rather than exact replication. This method aligns the output distributions of teacher samples in a large memory buffer, improving the robustness and performance of the student model without the need for strict negative instance differentiation. Our approach demonstrates superior performance on CIFAR-100, outperforming traditional KD techniques and surpassing 13 state-of-the-art methods. It also transfers successfully to other datasets like Tiny ImageNet and STL-10. The code will be made public soon.*

## 1. Introduction

Knowledge distillation (KD) is a technique that facilitates the transfer of knowledge from a larger, well-trained model (teacher) to a smaller, more efficient model (student). This is achieved by minimizing the Kullback-Leibler (KL) divergence between their outputs, allowing the student model to approximate the performance of the teacher model while maintaining lower computational complexity. This process is particularly beneficial for deployment in resource-constrained environments. A critical aspect of KD is representation learning, which enables the student model to acquire meaningful feature representations that capture the underlying data distribution. Effective representation learning in KD can significantly boost the performance of

the student model across various domains, such as natural language processing, computer vision, and speech recognition [10, 15, 22]. Despite these advantages, a major challenge in KD is the efficient transfer of complex knowledge from the teacher to the student model. Ensuring that the student model captures the abstract features and nuanced information present in the teacher model, without the need for similar computational capacity, remains a significant bottleneck.

Recent advancements in KD have introduced various strategies to enhance the transfer process, addressing the bottlenecks associated with representation learning. Techniques such as adversarial training, attention transfer, and contrastive representation distillation have been proposed to further align the representations learned by the student model with those of the teacher model. Adversarial training involves using adversarial examples to improve the robustness of the student model, while attention transfer focuses on aligning the attention maps of the teacher and student models to ensure that both models focus on similar regions of the input data [26, 32]. Contrastive representation distillation aims to improve the quality of learned representations by encouraging the student model to produce similar representations for similar inputs while differentiating dissimilar inputs. Additionally, methods like BookKD reduce distillation costs by decoupling knowledge generation and learning processes, leading to improved performance with minimal resource consumption [36]. Other approaches like structured KD focus on training compact networks by distilling structured knowledge from cumbersome networks [15]. These methods aim to capture richer information from the teacher model, leading to more robust and generalized student models. The continuous evolution of KD techniques underscores its pivotal role in developing efficient deep learning models capable of high performance with lower computational costs, while overcoming the challenges of effective knowledge transfer.

Our proposed method, Relational Representation Distillation (RRD), introduces a novel approach to address these challenges by maintaining relational consistency between the teacher and student models. By leveraging a large memory buffer of teacher samples to align their output distributions,

our method ensures consistent relational structures, thereby enhancing the robustness and performance of the student model.

Our contributions are threefold:

1. We propose a novel relational consistency framework for KD that leverages a memory buffer to maintain relational structures between teacher and student models.
2. We introduce a relational consistency loss that aligns the similarity distributions of teacher and student outputs, improving the robustness and generalization of the student model.
3. We validate the effectiveness of RRD through comprehensive testing on standard benchmarks, showcasing considerable gains in both accuracy and robustness. RRD surpasses other methods with a 19.22% relative improvement<sup>1</sup> over conventional KD. When integrated with KD, it demonstrates a 55.18% relative improvement over standard KD, underscoring its robust potential in enhancing model performance significantly.

The rest of this paper is organized as follows. Section 2 reviews related work in KD and contrastive learning. Section 3 details our proposed methodology. Section 4 presents our experimental setup and results, and Section 5 concludes the paper.

## 2. Related Work

The study of [10] on KD introduced the idea of transferring knowledge from large, complex models to smaller, more efficient models without losing their generalization capabilities. This technique involves temperature scaling in the softmax outputs to effectively capture and convey the knowledge from the teacher model. Numerous enhancements to this method have been proposed. For example, using intermediate representations or "hints" to guide the learning process [22], and aligning the attention maps of teacher and student models to ensure they focus on similar areas during training [32]. Other methods preserve relational knowledge between samples [28] or align the correlation structures between teacher and student models [20]. Additionally, some techniques use variational inference to improve the knowledge transfer process [1]. Further developments include focusing on structural relationships between data points to ensure the student model learns relational information [18], and maintaining the internal dynamics of neural networks during distillation [9, 19]. Other notable techniques include

<sup>1</sup>Average relative improvement is calculated as:  $\frac{1}{N} \sum_{i=1}^N \frac{\text{Acc}^i \text{RRD} - \text{Acc}^i \text{KD}}{\text{Acc}^i \text{KD} - \text{Acc}^i \text{van}}$ , where  $\text{Acc}^i \text{RRD}$ ,  $\text{Acc}^i \text{KD}$ , and  $\text{Acc}^i \text{van}$  represent the accuracies of RRD, KD, and vanilla training of the  $i$ -th student model, respectively [27].

network compression through factor transfer [12], optimizing networks for better transfer learning [31], promoting selectivity in the distillation process [11], and using contrastive learning objectives to enhance representation learning [27].

Self-supervised learning has significantly impacted representation learning by leveraging unlabeled data. Methods such as SimCLR [3] and MoCo [7] use contrastive losses to learn useful representations by maximizing agreement between different augmented views of the same data point. ReSSL [35] introduces relational self-supervised learning, which explores the relationships between data points. These approaches have inspired various KD methods, including our proposed method, which adapts relational consistency from self-supervised learning to the KD framework.

Our method, RRD, differentiates itself from state-of-the-art methods by focusing on maintaining relational consistency between the teacher and student models. Unlike traditional KD methods that often rely on direct alignment of logits or intermediate features, RRD leverages a large memory buffer of teacher samples to align the relational structures of the output distributions. This approach not only enhances the robustness and performance of the student model but also provides a more flexible and scalable solution for KD.

## 3. Methodology

This section presents our methodology to improve the efficiency and accuracy of KD. Our method, Relational Representation Distillation (RRD), focuses on maintaining relational consistency between the teacher and student models by leveraging a large memory buffer of teacher samples to align their output distributions. By ensuring consistent relational structures, RRD enhances the robustness and performance of the student model. Figure 1 shows an overview of the proposed RRD method.

### 3.1. Preliminary

KD involves transferring knowledge from a high-capacity teacher neural network, denoted as  $f^T$ , to a more compact student neural network,  $f^S$ . Consider  $x_i$  as the input to these networks, typically an image. We represent the outputs at the penultimate layer (just before the final classification layer, or logits) as  $z_i^T = f^T(x_i)$  and  $z_i^S = f^S(x_i)$  for the teacher and student models, respectively. The primary objective of KD is to enable the student model to approximate the performance of the teacher model while leveraging the student's computational efficiency. The overall distillation process can be mathematically expressed as:

$$\mathcal{L} = \mathcal{L}_{\text{sup}}(y_i, z_i^S) + \lambda \cdot \mathcal{L}_{\text{distill}}(z_i^T, z_i^S) \quad (1)$$

where  $y_i$  represents the true label for the input  $x_i$  and  $\lambda$  is a hyperparameter that balances the supervised loss and the distillation loss. The loss  $\mathcal{L}_{\text{sup}}$  is the alignment error between

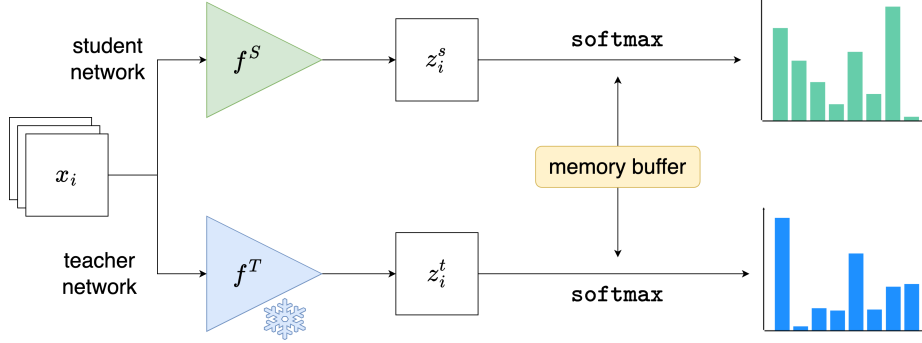


Figure 1. Overview of the RRD method. The student network processes input  $x_i$  to produce embeddings  $z_i^S$ , while the teacher network, indicated as frozen by a snowflake, processes the same input to generate embeddings  $z_i^T$ . The embeddings are stored in a memory buffer to align their output distributions via softmax layers. The relational consistency between the teacher and student models is enforced by leveraging the stored embeddings to train the student network.

the network prediction and the annotation. For example, in the image classification task [4, 17, 21, 24], it is normally a cross-entropy loss. For object detection [2, 14], it includes bounding box regression as well. The loss  $\mathcal{L}_{\text{distill}}$  is the mimic error of the student network towards a pre-trained teacher network, typically implemented as KL divergence between student and teacher outputs [10].

### 3.2. Relational consistency

Our method is inspired by self-supervised learning. Traditional contrastive self-supervised learning uses instance discrimination as a pretext task and relies on  $(K+1)$ -softmax classification, where different instances are pushed apart, and augmented views of the same instance are expected to have identical features. Applying such properties to KD imposes overly strict constraints, where a contrastive loss encourages the representations from the teacher and student models for the same input data to be similar, while simultaneously pushing apart representations from different data inputs:

$$\mathcal{L}_{\text{contrast}}(z_i^T, z_i^S) = -\log \frac{\exp(\phi(z_i^T, z_i^S)/\tau)}{\sum_{j=1}^M \exp(\phi(z_i^S, z_j^T)/\tau)} \quad (2)$$

where  $\mathcal{L}_{\text{contrast}}$  is the InfoNCE [29] loss, typically employed in self-supervised methods,  $\phi$  is a similarity function,  $\tau$  is a temperature parameter, and  $M$  is the number of negative samples.

In this way, we do not encourage explicit negative instances (those to be pushed away) for each instance; instead, we leverage the pairwise similarities to explore their relationships. We pull the features of the student  $f^S$  and teacher  $f^T$ . As a result, our method relaxes Equation (2), where different teacher and student outputs do not always need to be pushed away from each other; and teacher and student need to share similar but not exactly the same features.

Concretely, given an input image  $x_i$ , and the outputs  $z_i^T = f^T(x_i)$  and  $z_i^S = f^S(x_i)$  for the teacher and student models, respectively, we calculate their similarity measured by  $\phi(z_i^T, z_i^S)$ . A softmax layer can be adopted to process the calculated similarities, which then produces a relationship distribution:

$$p_i^T = \frac{\exp(\phi(z_i^T, z_j^T)/\tau_t)}{\sum_{k=1}^M \exp(\phi(z_i^T, z_k^T)/\tau_t)} \quad (3)$$

where  $\tau_t$  is the temperature parameter for the teacher network. At the same time, we can calculate the relationship distribution for the student model as:

$$p_i^S = \frac{\exp(\phi(z_i^S, z_j^S)/\tau_s)}{\sum_{k=1}^M \exp(\phi(z_i^S, z_k^S)/\tau_s)} \quad (4)$$

where  $\tau_s$  is a different temperature parameter for the student network. We propose to push the relational consistency between  $p_i^T$  and  $p_i^S$ , similar to [35], by minimizing the KL divergence, which can be formulated as:

$$\mathcal{L}_{\text{relational}}(z_i^T, z_i^S) = KL(p_i^T \parallel p_i^S) = H(p_i^T, p_i^S) - H(p_i^T) \quad (5)$$

where  $KL$  denotes the KL divergence between  $p_i^T$  and  $p_i^S$ . Since  $p_i^T$  will be used as a target, the gradient will be clipped here to avoid the model collapsing, thus we only minimize the cross-entropy term  $H(p_i^T, p_i^S)$  in our implementation.

However, the quality of the target similarity distribution  $p_i^T$  is crucial for reliable and stable training. To ensure this, we maintain a large memory buffer  $Q$ , storing the feature embeddings from teacher batches. The relational consistency between the teacher and student models is enforced by aligning the similarity distributions of their outputs using the KL divergence.

We normalize the outputs  $z_i^T$  and  $z_i^S$  before computing the loss, ensuring that the representations lie on a unit hypersphere. To compute  $\mathcal{L}_{\text{relational}}$ , we further encode  $z_i^T$  and  $z_i^S$  using a projection head to match the dimensions. This ensures that the representations from both models are compatible for comparison and alignment.

The final objective function, which includes the supervised loss and standard KL divergence, is given by:

$$\mathcal{L} = \mathcal{L}_{\text{sup}}(y_i, z_i^S) + \lambda \cdot \mathcal{L}_{\text{distill}}(z_i^T, z_i^S) + \beta \cdot \mathcal{L}_{\text{relational}}(z_i^T, z_i^S) \quad (6)$$

where  $\beta$  is a hyperparameter that balances the KD loss  $\mathcal{L}_{\text{relational}}$ . We experiment with  $\beta$  in ablation studies to understand its impact on the final performance.

## 4. Experiments

We evaluate our RRD framework in the KD task of model compression of a large network to a smaller one.

**Datasets.** (1) CIFAR-100 [13] contains 50,000 training images with 500 images per class and 10,000 test images. (2) STL-10 [5] consists of a training set of 5,000 labeled images from 10 classes and 100,000 unlabeled images, and a test set of 8,000 images. (3) Tiny ImageNet (TIN-200) [6] has 200 classes, each with 500 training images and 50 validation images.

**Setup.** We experiment on CIFAR-100 with student-teacher combinations of various capacity, such as ResNet [8] or Wide ResNet (WRN) [33], VGG [25], MobileNet [23], and ShuffleNet [16, 34] (more details about the network architectures are described in the supplementary material). We use  $M = 16384$  negative samples and set the temperature parameter of the student to  $\tau_s = 0.04$  and of the teacher to  $\tau_t = 0.07$ . Both the student and teacher outputs are projected to a 128-dimensional space. We use a projection head of a single linear layer, followed by  $\ell_2$  normalization. We train for a total of 240 epochs. More details on the training details are described in the supplementary material.

### 4.1. Results on CIFAR-100

Table 1 and Table 2 present the top-1 accuracies of student networks trained using different distillation techniques across various teacher-student architectural pairings. Table 1 examines pairings where both student and teacher models share similar architectural styles, while Table 2 focuses on cross-architecture distillations. Our proposed loss consistently outperforms the conventional KD technique, as indicated by the green upward arrows ( $\uparrow$ ). While the standalone performance of our method is comparable to CRD, its integration with KD not only achieves higher accuracies but in some cases, surpasses the performance of the teacher networks, such as in the distillation of WRN-40-2 to ShuffleNet-v1. The enhanced performance of our distillation

method can be credited to multiple factors that collectively improve the transfer of knowledge from the teacher to the student model. Our approach uses a unique loss function that complements KD’s primary focus on matching the softened output logits of the teacher and student. We introduce an additional layer of representational alignment that ensures not only the final outputs but also the intermediate feature representations of the student closely match those of the teacher. This dual focus allows the student model to mimic the teacher’s outputs and develop more robust and generalizable internal representations.

### 4.2. Capturing inter-class correlations

Cross-entropy loss overlooks the relationships among class logits in a teacher network, often resulting in less effective knowledge transfer. Distillation techniques that use "soft targets", such as those described by [10], have successfully captured these relationships, improving student model performance. Figure 4 assesses the effectiveness of different distillation methods on the CIFAR-100 KD task using WRN-40-2 as the teacher and WRN-40-1 as the student. We compare students trained without distillation, with attention transfer [32], with KL divergence [10], and with our proposed RRD method. Our findings show that RRD achieves close alignment between teacher and student logits, as evidenced by reduced differences in their correlation matrices. While RRD does not match CRD [27] in terms of exact correlation alignment, it significantly enhances learning efficiency and reduces error rates. The smaller discrepancies between teacher and student logits indicate that the RRD objective captures a substantial portion of the correlation structure in the logits, resulting in lower error rates, though CRD achieves a slightly closer match.

### 4.3. Transferability of representations

Our study investigates how knowledge is transferred from a larger teacher network (WRN-40-2) to a smaller student network (WRN-16-2), aiming to develop versatile representations suitable for a range of tasks and datasets. We apply this technique by having the student network either learn directly from the CIFAR-100 dataset or via distillation. In this setup, the student network is employed as a static feature extractor for images from the STL-10 and TIN-200 datasets, both adjusted to a  $32 \times 32$  resolution. We evaluate the adaptability of these features by training a linear classifier on the final feature layer to conduct classifications with 10 categories for STL-10 and 200 categories for TIN-200. We document the impact of various distillation approaches on the transferability of these features in Table 3. Our findings reveal that, except for the FitNet method, all distillation techniques significantly improve the feature transferability on both datasets. Notably, while the teacher network achieves the highest performance on CIFAR-100, its features show

Teacher	WRN-40-2	WRN-40-2	resnet-56	resnet-110	resnet-110	resnet-32x4	VGG-13
Student	WRN-16-2	WRN-40-1	resnet-20	resnet-20	resnet-32	resnet-8x4	VGG-8
Teacher	75.61	75.61	72.34	74.31	74.31	79.42	74.64
Student	73.26	71.98	69.06	69.06	71.14	72.50	70.36
KD	74.92	73.54	70.66	70.67	73.08	73.33	72.98
FitNet	73.58 (↓)	72.24 (↓)	69.21 (↓)	68.99 (↓)	71.06 (↓)	73.50 (↓)	71.02 (↓)
AT	74.08 (↓)	72.77 (↓)	70.55 (↓)	70.22 (↓)	72.31 (↓)	73.44 (↓)	71.43 (↓)
SP	73.83 (↓)	72.43 (↓)	69.67 (↓)	70.04 (↓)	72.69 (↓)	72.94 (↓)	72.68 (↓)
CC	73.56 (↓)	72.21 (↓)	69.63 (↓)	69.48 (↓)	71.48 (↓)	72.97 (↓)	70.81 (↓)
VID	74.11 (↓)	73.30 (↓)	70.38 (↓)	70.16 (↓)	72.61 (↓)	73.09 (↓)	71.23 (↓)
RKD	73.35 (↓)	72.22 (↓)	69.61 (↓)	69.25 (↓)	71.82 (↓)	71.90 (↓)	71.48 (↓)
PKT	74.54 (↓)	73.45 (↓)	70.34 (↓)	70.25 (↓)	72.61 (↓)	73.64 (↑)	72.88 (↓)
AB	72.50 (↓)	72.38 (↓)	69.47 (↓)	69.53 (↓)	70.98 (↓)	73.17 (↓)	70.94 (↓)
FT	73.25 (↓)	71.59 (↓)	69.84 (↓)	70.22 (↓)	72.37 (↓)	72.86 (↓)	70.58 (↓)
FSP	72.91 (↓)	n/a	69.95 (↓)	70.11 (↓)	71.89 (↓)	72.62 (↓)	70.33 (↓)
NST	73.68 (↓)	72.24 (↓)	69.60 (↓)	69.53 (↓)	71.96 (↓)	73.30 (↓)	71.53 (↓)
CRD	75.48 (↑)	74.14 (↑)	71.16 (↑)	71.46 (↑)	73.48 (↑)	<b>75.51</b> (↑)	73.94 (↑)
CRD+KD	75.64 (↑)	<b>74.38</b> (↑)	71.63 (↑)	71.56 (↑)	<b>73.75</b> (↑)	75.46 (↑)	74.29 (↑)
RRD	75.01 (↑)	73.55 (↑)	70.71 (↑)	70.72 (↑)	73.10 (↑)	74.21 (↑)	73.99 (↑)
RRD+KD	<b>75.66</b> (↑)	73.77 (↑)	<b>71.72</b> (↑)	<b>71.62</b> (↑)	73.48 (↑)	74.86 (↑)	<b>74.32</b> (↑)

Table 1. Test top-1 accuracy (%) of student networks on CIFAR-100, comparing students and teachers of the same architecture using various distillation methods. ↑ denotes outperformance over KD and ↓ denotes underperformance. Results adapted from [27]. The citations and abbreviations of other methods are described in the supplementary material. The values in bold indicate the maximum of each column.

Teacher	VGG-13	ResNet-50	ResNet-50	ResNet-32x4	ResNet-32x4	WRN-40-2
Student	MobileNet-v2	MobileNet-v2	VGG-8	ShuffleNet-v1	ShuffleNet-v2	ShuffleNet-v1
Teacher	74.64	79.34	79.34	79.42	79.42	75.61
Student	64.6	64.6	70.36	70.5	71.82	70.5
KD	67.37	67.35	73.81	74.07	74.45	74.83
FitNet	64.14 (↓)	63.16 (↓)	70.69 (↓)	73.59 (↓)	73.54 (↓)	73.73 (↓)
AT	59.40 (↓)	58.58 (↓)	71.84 (↓)	71.73 (↓)	72.73 (↓)	73.32 (↓)
SP	66.30 (↓)	68.08 (↓)	73.34 (↓)	73.48 (↓)	74.56 (↑)	74.52 (↓)
CC	64.86 (↓)	65.43 (↓)	70.25 (↓)	71.14 (↓)	71.29 (↓)	71.38 (↓)
VID	65.56 (↓)	67.57 (↓)	70.30 (↓)	73.38 (↓)	73.40 (↓)	73.61 (↓)
RKD	64.52 (↓)	64.43 (↓)	71.50 (↓)	72.28 (↓)	73.21 (↓)	72.21 (↓)
PKT	67.13 (↓)	66.52 (↓)	73.01 (↓)	74.10 (↑)	74.69 (↑)	73.89 (↓)
AB	66.06 (↓)	67.20 (↓)	70.65 (↓)	73.55 (↓)	74.31 (↓)	73.34 (↓)
FT	61.78 (↓)	60.99 (↓)	70.29 (↓)	71.75 (↓)	72.50 (↓)	72.03 (↓)
NST	58.16 (↓)	64.96 (↓)	71.28 (↓)	74.12 (↑)	74.68 (↑)	76.09 (↑)
CRD	69.73 (↑)	69.11 (↑)	74.30 (↑)	75.11 (↑)	75.65 (↑)	76.05 (↑)
CRD+KD	69.94 (↑)	<b>69.54</b> (↑)	<b>74.58</b> (↑)	<b>75.12</b> (↑)	<b>76.05</b> (↑)	76.27 (↑)
RRD	67.93 (↑)	68.84 (↑)	74.01 (↑)	74.11 (↑)	74.64 (↑)	74.98 (↑)
RRD+KD	<b>69.98</b> (↑)	69.13 (↑)	74.26 (↑)	74.78 (↑)	75.78 (↑)	<b>76.31</b> (↑)

Table 2. Test top-1 accuracy (%) of student networks on CIFAR-100 involving students and teachers from different architectures, using various distillation methods. ↑ denotes outperformance over KD and ↓ denotes underperformance. Results adapted from [27]. The citations and abbreviations of other methods are described in the supplementary material. The values in bold indicate the maximum of each column.

the least effective transfer, likely due to training data specificity. Conversely, the student network using a combination of RRD and KD distillation techniques not only equates to the teacher’s CIFAR-100 performance but also surpasses it

in transferability, showing improvements of 3.4% and 2.1% in STL-10 and TIN-200 respectively.

	Teacher	Student	KD	AT	FitNet	CRD	CRD+KD	RRD	RRD+KD
CIFAR-100→STL-10	68.6	69.7	70.9	70.7	70.3	71.6	<b>72.2</b>	71.2	72.0
CIFAR-100→TIN-200	31.5	33.7	33.9	34.2	33.5	<b>35.6</b>	35.5	34.8	35.0

Table 3. Test top-1 accuracy (%) of WRN-16-2 (student) distilled from WRN-40-2 (teacher). In this setup, the representations learned from the CIFAR-100 dataset are transferred to the STL-10 and TIN-200 datasets. The network is frozen, and a linear classifier is trained on the last feature layer to perform classification with 10 classes (STL-10) or 200 classes (TIN-200). Results adapted from [27]. The values in bold indicate the maximum of each row.

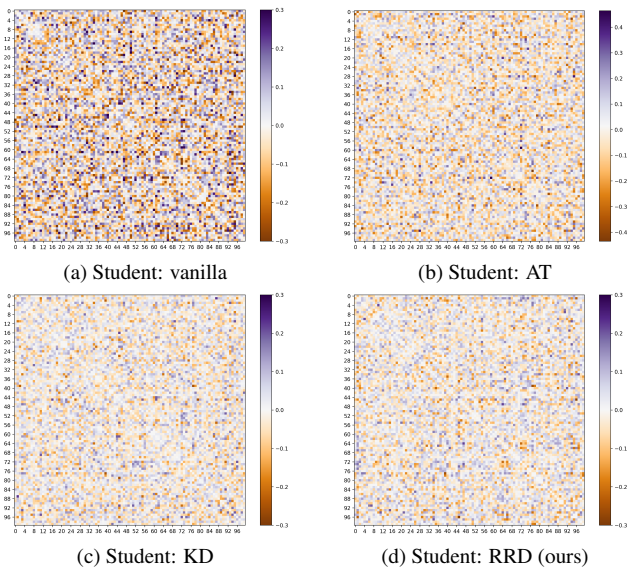


Figure 2. Comparison of correlation matrix differences between teacher and student logits across various distillation methods on the CIFAR-100 task. Subfigures show results for (a) students trained without distillation, (b) with attention transfer [32], (c) with KL divergence [10], and (d) with our RRD method, highlighting better matching between student’s and teacher’s correlations. Results have been re-implemented according to [27].

#### 4.4. Visualization of t-SNE embeddings

We provide t-SNE [30] visualizations to compare the embeddings generated by various KD methods and the teacher network on the CIFAR-100 dataset. Figure 3 displays the embeddings from the teacher network, a WRN-40-2, and the student network, WRN-40-1, under standard training as well as distillation using AT and RRD where we limit the dataset to the first 10 classes of CIFAR-100 to offer a clearer understanding of the embedding space. We observe improved consistency in the embedding distributions between the teacher and student networks, indicating that RRD effectively transfers the knowledge of the teacher’s feature space to the student. Our relational consistency approach ensures that the spatial relationships in the embedding spaces of both the student and teacher models are preserved. This alignment not only enhances the student’s performance but

also maintains the integrity of the feature representations learned by the teacher.

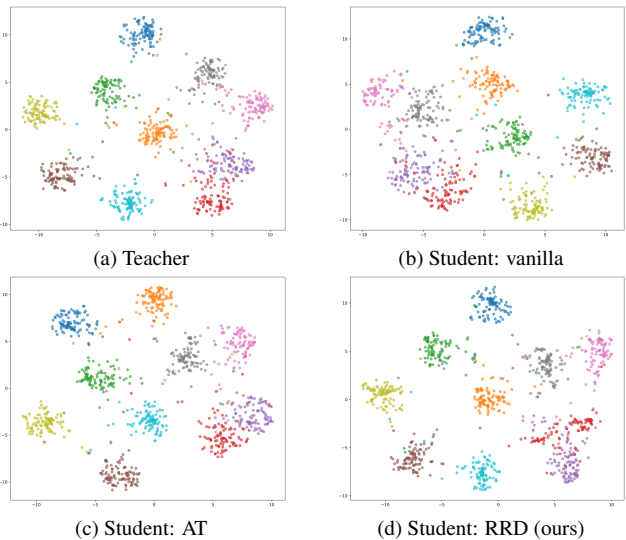


Figure 3. t-SNE visualizations of embeddings from the teacher network and student networks trained using different distillation techniques on the first 10 classes of the CIFAR-100 dataset.

#### 4.5. Ablation study

There are two main hyperparameters in our objective: the number of negative samples  $M$  in the memory buffer  $Q$  of Equation (3) and Equation (4); and temperature parameters  $\tau_s$  and  $\tau_t$  of Equation (3) and Equation (4) that modulate the softmax probability. We also ablate the hyperparameter  $\beta$  that balances the KD loss. For the ablation study, we adopt WRN-40-2 as the teacher and WRN-16-2 as the student. Experiments are conducted on CIFAR-100, and the results are shown in Figure 4.

**Number of negatives  $M$ .** We validated different values for  $M$ : 256, 1024, 2048, 4096, 8192, 16384, and 32768. As shown in Figure 4a, increasing  $M$  leads to improved performance. However, the difference in error rate between  $M = 4096$  and  $M = 16384$  is less than 0.5%. Therefore, we use  $M = 16384$  for reporting the accuracy, while in practice lower  $M$  should suffice. Going beyond  $M = 16384$  proves to harm performance.

**Temperature  $\tau_s$  and  $\tau_t$ .** We varied  $\tau_s$  and  $\tau_t$ , considering all the permutations of the numbers 0.04, 0.07, and 0.2 taken two at a time, considering that order matters. As Figure 4b illustrates, both extremely high or low temperatures lead to a sub-optimal solution. Also, as expected, a lower  $\tau_s$  than  $\tau_t$  leads to better performance. This improvement is attributed to the sharper predictions from the student model with a lower temperature, resulting in more confident and distinct class probabilities. This sharpness helps the student model align better with the teacher’s guidance, enhance generalization, provide a more informative learning signal, and reduce overfitting. The sweep spot lies at  $\tau_s = 0.04$  and  $\tau_t = 0.07$  (red area of Figure 4b).

**Loss coefficient  $\beta$ .** We varied  $\beta$  from 0.1 to 100. As Figure 4c illustrates, both extremely high or low  $\beta$  lead to a sub-optimal solution. In general,  $\beta$  between 1 and 2 works well on CIFAR-100.

**Computational Cost.** The RRD loss method introduces an additional 5.24 MFLOPs to the computational workload of a ResNet-50 model. This represents approximately 0.262% of the original 2 GFLOPs computational baseline. Despite the added computational complexity, the impact on training time is minimal, allowing us to maintain efficiency in practical training scenarios such as on CIFAR-100. The memory bank for RRD stores all 128-dimensional features of up to 16,384 CIFAR-100 images, consuming about 8 MB of GPU memory.

## 5. Conclusions

Our method offers a significant advancement in KD by maintaining relational consistency between teacher and student models. RRD leverages a large memory buffer of teacher samples to align their output distributions, ensuring consistent relational structures throughout the learning process. Unlike traditional approaches, RRD uses pairwise similarities and a relaxed contrastive loss to enhance the robustness and performance of the student model without explicit negative instances. Through comprehensive testing on CIFAR-100, TIN-200, and STL-10 datasets, RRD consistently outperforms traditional KD techniques and state-of-the-art methods, demonstrating substantial improvements in accuracy, robustness, and transferability of learned representations. Our experiments on model compression highlight RRD’s ability to provide a scalable solution.

## References

- [1] Sungsoo Ahn, Shell Xu Hu, Andreas Damianou, Neil D Lawrence, and Zhenwen Dai. Variational information distillation for knowledge transfer. In *Proceedings of the IEEE Conference on Computer Vision and Pattern Recognition*, pages 9163–9171, 2019. 2
- [2] Gongfan Chen, Yuting Wang, Jiajun Xu, Zhe Du, Qionghai Dai, Shiyang Geng, and Tao Mei. Learning efficient object detection models with knowledge distillation. In *Advances in Neural Information Processing Systems*, pages 742–751, 2017. 3
- [3] Ting Chen, Simon Kornblith, Mohammad Norouzi, and Geoffrey Hinton. A simple framework for contrastive learning of visual representations, 2020. 2
- [4] Jang Hyun Cho and Bharath Hariharan. On the efficacy of knowledge distillation. In *Proceedings of the IEEE/CVF International Conference on Computer Vision*, pages 4794–4802, 2019. 3
- [5] Adam Coates and Andrew Y. Ng. The importance of encoding versus training with sparse coding and vector quantization. In *Proceedings of the 28th International Conference on International Conference on Machine Learning, ICML’11*, page 921–928, Madison, WI, USA, 2011. Omnipress. 4
- [6] Jia Deng, Wei Dong, Richard Socher, Li-Jia Li, K. Li, and Li Fei-Fei. Imagenet: A large-scale hierarchical image database. *2009 IEEE Conference on Computer Vision and Pattern Recognition*, pages 248–255, 2009. 4
- [7] Kaiming He, Haoqi Fan, Yuxin Wu, Saining Xie, and Ross Girshick. Momentum contrast for unsupervised visual representation learning, 2020. 2
- [8] Kaiming He, Xiangyu Zhang, Shaoqing Ren, and Jian Sun. Deep residual learning for image recognition, 2015. 4
- [9] Byeongho Heo, Minsik Lee, Seong Joon Yun, Jin Young Choi, and In So Kweon. Knowledge transfer via distillation of activation boundaries formed by hidden neurons. In *Proceedings of the AAAI Conference on Artificial Intelligence*, pages 3779–3787, 2019. 2
- [10] Geoffrey Hinton, Oriol Vinyals, and Jeff Dean. Distilling the knowledge in a neural network, 2015. 1, 2, 3, 4, 6
- [11] Zehao Huang and Naiyan Wang. Like what you like: Knowledge distill via neuron selectivity transfer. In *Advances in Neural Information Processing Systems*, pages 185–195, 2017. 2
- [12] Jangho Kim, Seongwon Park, and Nojun Kwak. Paraphrasing complex network: Network compression via factor transfer. In *Advances in Neural Information Processing Systems*, pages 2760–2769, 2018. 2
- [13] Alex Krizhevsky. Learning multiple layers of features from tiny images. pages 32–33, 2009. 4
- [14] Wei Liu, Andrew Rabinovich, and Alexander C Berg. Learning efficient single-stage pedestrian detectors by asymptotic localization fitting. In *Proceedings of the European Conference on Computer Vision (ECCV)*, pages 618–634, 2018. 3
- [15] Yifan Liu, Ke Chen, Chris Liu, Zengchang Qin, Zhenbo Luo, and Jingdong Wang. Structured knowledge distillation for semantic segmentation. In *Proceedings of the IEEE Conference on Computer Vision and Pattern Recognition (CVPR)*, pages 2604–2613, 2019. 1
- [16] Ningning Ma, Xiangyu Zhang, Hai-Tao Zheng, and Jian Sun. Shufflenet v2: Practical guidelines for efficient cnn architecture design. In *Proceedings of the European Conference on Computer Vision (ECCV)*, pages 116–131, 2018. 4
- [17] Arun Mishra and Debbie Marr. Apprentice: Using knowledge distillation techniques to improve low-precision network

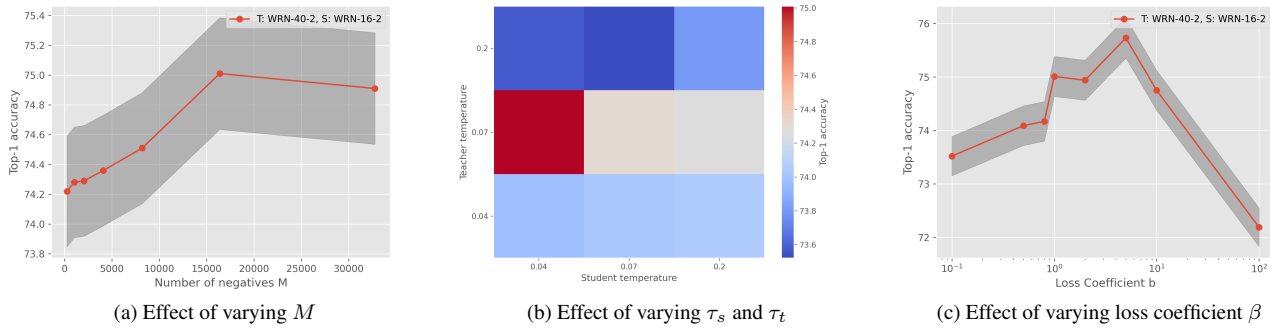


Figure 4. Ablation study results on CIFAR-100 using WRN-40-2 as the teacher and WRN-16-2 as the student. (a) Effect of the number of negatives  $M$  on performance. Increasing  $M$  generally improves performance, but the difference becomes negligible beyond  $M = 4096$ . (b) Effect of temperature parameters  $\tau_s$  and  $\tau_t$ . Lower  $\tau_s$  than  $\tau_t$  results in better performance, with extremely high or low temperatures leading to sub-optimal solutions. (c) Effect of loss coefficient  $\beta$  on performance (logarithmic scale). Optimal  $\beta$  values range between 1 and 2.

- accuracy. In *International Conference on Learning Representations*, 2017. 3
- [18] Wonpyo Park, Dongju Kim, Yan Lu, and Minsu Cho. Relational knowledge distillation. In *Proceedings of the IEEE Conference on Computer Vision and Pattern Recognition*, pages 3967–3976, 2019. 2
- [19] Nikolaos Passalis and Anastasios Tefas. Learning deep representations with probabilistic knowledge transfer. In *Proceedings of the European Conference on Computer Vision (ECCV)*, pages 268–284, 2018. 2
- [20] Baoyun Peng, Xi Li, Yifan Wu, Yizhou Fan, Bo Wang, Qi Tian, and Jun Liang. Correlation congruence for knowledge distillation. In *Proceedings of the IEEE International Conference on Computer Vision*, pages 5007–5016, 2019. 2
- [21] Antonio Polino, Razvan Pascanu, and Dan Alistarh. Model compression via distillation and quantization. In *International Conference on Learning Representations*, 2018. 3
- [22] Adriana Romero, Nicolas Ballas, Samira Ebrahimi Kahou, Antoine Chassang, Carlo Gatta, and Yoshua Bengio. Fitnets: Hints for thin deep nets. In *Proceedings of the 4th International Conference on Learning Representations*, 2014. 1, 2
- [23] Mark Sandler, Andrew Howard, Menglong Zhu, Andrey Zhmoginov, and Liang-Chieh Chen. Mobilenetv2: Inverted residuals and linear bottlenecks. In *Proceedings of the IEEE conference on computer vision and pattern recognition*, pages 4510–4520, 2018. 4
- [24] Li Shen and Marios Savvides. Amalgamating knowledge towards comprehensive classification. In *Proceedings of the IEEE/CVF Conference on Computer Vision and Pattern Recognition*, pages 1687–1696, 2020. 3
- [25] Karen Simonyan and Andrew Zisserman. Very deep convolutional networks for large-scale image recognition, 2015. 4
- [26] Yonglong Tian, Dilip Krishnan, and Phillip Isola. Contrastive multiview coding, 2020. 1
- [27] Yonglong Tian, Dilip Krishnan, and Phillip Isola. Contrastive representation distillation, 2022. 2, 4, 5, 6
- [28] Frederick Tung and Greg Mori. Similarity-preserving knowledge distillation. In *Proceedings of the IEEE International Conference on Computer Vision*, pages 1365–1374, 2019. 2
- [29] Aaron van den Oord, Yazhe Li, and Oriol Vinyals. Representation learning with contrastive predictive coding, 2019. 3
- [30] Laurens van der Maaten and Geoffrey Hinton. Visualizing data using t-sne. *Journal of Machine Learning Research*, 9(Nov):2579–2605, 2008. 6
- [31] Junho Yim, Donggyu Joo, Jihoon Bae, and Junmo Kim. A gift from knowledge distillation: Fast optimization, network minimization and transfer learning. In *Proceedings of the IEEE Conference on Computer Vision and Pattern Recognition*, pages 4133–4141, 2017. 2
- [32] Sergey Zagoruyko and Nikos Komodakis. Paying more attention to attention: Improving the performance of convolutional neural networks via attention transfer. In *Proceedings of the 5th International Conference on Learning Representations*, 2016. 1, 2, 4, 6
- [33] Sergey Zagoruyko and Nikos Komodakis. Wide residual networks, 2017. 4
- [34] Xiangyu Zhang, Xinyu Zhou, Mengxiao Lin, and Jian Sun. Shufflenet: An extremely efficient convolutional neural network for mobile devices. In *Proceedings of the IEEE conference on computer vision and pattern recognition*, pages 6848–6856, 2018. 4
- [35] Mingkai Zheng, Shan You, Fei Wang, Chen Qian, Changshui Zhang, Xiaogang Wang, and Chang Xu. Rssl: Relational self-supervised learning with weak augmentation, 2021. 2, 3
- [36] Songling Zhu, Ronghua Shang, Ke Tang, Songhua Xu, and Yangyang Li. Bookkd: A novel knowledge distillation for reducing distillation costs by decoupling knowledge generation and learning. *Knowledge-Based Systems*, 263:110916, 2023. 1